Available online at www.sciencedirect.com

ScienceDirect

IFAC Papers Online CONFERENCE PAPER ARCHIVE

IFAC-PapersOnLine 48-1 (2015) 427–432

A Combined Methodology for Studying the Axial Balancing Mechanism of Orbit Annular Hydraulic Machines

Elisa Bigliardi*, Marco Francia, Massimo Milani***, Luca Montorsi****, Fabrizio Paltrinieri*****, Matteo Stefani********

** DISMI - University of Modena and Reggio Emilia, Reggio Emilia, 42122 Italy (e-mail: elisa.bigliardi@unimore.it)*
*** DISMI - University of Modena and Reggio Emilia, Reggio Emilia, 42122 Italy (e-mail: marco.francia@unimore.it)*
**** DISMI - University of Modena and Reggio Emilia, Reggio Emilia, 42122 Italy (Tel: +39 0522 52 3501; e-mail: massimo.milani@unimore.it)*
***** DISMI - University of Modena and Reggio Emilia, Reggio Emilia, 42122 Italy (Tel: +39 0522 52 3502; e-mail: luca.montorsi@unimore.it)*
****** DISMI - University of Modena and Reggio Emilia, Reggio Emilia, 42122 Italy (Tel: +39 0522 52 3503; e-mail: fabrizio.paltrinieri@unimore.it)*
******* DISMI - University of Modena and Reggio Emilia, Reggio Emilia, 42122 Italy (e-mail: matteo.stefani@unimore.it)*

Abstract: A customized combined methodology, based on both 2D CFD and lumped parameters numerical modeling, useful for simulating the hydraulic behavior of orbit annular machines, has been developed and here presented. More in details, the predictive capabilities of this CAE tool can be applied for the study of both roller and gerotor architectures and considering both pumping and motoring operating mode. First of all, a in-house developed 2D CFD methodology, based on the integration of the stationary form of the Reynolds equation for the determination of the pressure distribution inside the lateral clearances bounded by the sides of the stator-rotor group and the valve plate, as well as the internal manifold surface, is firstly presented and applied. The same computational procedure has been also involved for the investigation of the leakages through the clearance between the valve plate and the balancing ring. After that, a lumped and distributed parameters numerical model has been involved for the simulation of a typical orbit roller motor operation. In this case, particular care has been devoted to the modeling of the axial leakage clearances, adopting analytical interpolation functions deducted from the numerical results calculated applying the previously described 2D CFD methodology. Finally, the whole CAE approach has been validated by means of a comprehensive numerical vs. experimental comparison, obtaining a general good accordance for the overall operating field of this particular type of hydraulic unit.

Keywords: Hydraulic, Motor, Orbit, CFD, CAE, Reynolds.

1. INTRODUCTION

Technical and technological developments are continuously giving strong impulse to the performance improvement of hydraulic systems for industrial and mobile applications. Among others design aspects, particular attention has been devoted to the specific power and the overall efficiency increasing of the positive displacement units. This attention has deeply conditioned the design process in the field of mobile equipment applications, particular care has been dedicated to axial piston, external and internal gear pumps and motors. As well known, this design evolution determined a continuous increase in supply pressure operating level and a parallel decreasing of the units weight and volume.

The hydraulic machines designers have to face two main contrasting requirements: on one hand, the increasing of the motor supply mean operating pressure, on the other hand the contemporarily overall efficiency optimization.

Nowadays, hydraulically balanced orbit machines (shown in Fig. 1) represent a good design compromise in solving these problems and, thanks to the high density of power, they are commonly employed in many mobile applications.

During the last twenty years many contributions in this field have been proposed by several authors. For example, a simplified numerical model useful in determining the pressure transients in external gear pumps is presented and validated in Mancò et al. (1989) and in Mancò et al. (1993), while their journal bearing performance, their suction capabilities and the pressure transients within their meshing teeth are investigated in Gutés et al. (2000), Poy Ferrer et al. (2002) and Edge et al. (2001).

10.1016/j.ifacol.2015.05.110

Besides, in Koç et al. (1997a), Koç et al. (1997b) and Koç et al. (1997c) the lubrication mechanisms of positive displacement motors and pumps sealing gaps are illustrated, with particular attention given to the numerical and to the experimental analyses of the high pressure pumps bush-type bearings. These studies highlight the importance of the main motors and pumps components proper design, and in particular of the pressure balanced bearing blocks. The fluid dynamics behaviour of the sealing and bearing gaps are also deepened in many papers, where the attention has been devoted to the study both of the microscopic and macroscopic gap geometry (Lasaar (2000)) and of the thermal (Olems (2000)) and EHD (Huang (2002)) effects influence on energy dissipation. Finally, a reliable numerical method for the evaluation of the axial force in pressure compensated gears pumps and motors is presented in Bonacini et al. (1987).

In this paper an innovative CAE methodology based on both 2D CFD and lumped and distributed parameters numerical simulations has been built up and applied for studying and analyzing the operation of hydraulic roller motors. More in details, the predictive capabilities of the numerical procedure has been clearly demonstrated through a detailed comparison between computational results and experimental measurements gained from a testing campaign performed for a wide range of operating conditions in terms of both exerted torque levels and rotational speeds. Besides, the application of a customized 2D CFD model, based on the numerical integration of the Reynolds equation, permits to investigate the lubrication mechanism interesting the lateral clearances and to estimate the internal leakages of actual rotor-stator group of orbit roller motors. Then, the numerical results gathered from these CFD simulations have been adopted for calibrating the lumped and distributed parameters numerical model and thus for increasing the accuracy of the overall CAE procedure.

2. MACHINE LAYOUT

The annular gear pump, also called gerotor, is composed of an internal gear and a pinion, with the internally toothed annular gear having one tooth more than the pinion. As well known, the trochoidal shape of the line of contact ensures the sealing between the annular gear and the externally toothed pinion (Ivantysyn et al. (2003) and Merrit (1966)). Due to the meshing process, the individual displacement chambers are sealed against each other. During one revolution of the pinion the teeth of the externally toothed pinion alternately go down and up into the tooth spaces of the annular gear, thus the vane chamber is cyclically decreased and increased. This simple operating principle could be applied to design both pump or motor architectures.

In this work, the operating behaviour of a typical roller motor hydraulic unit (Fig. 1) has been studied and analysed by means of a customized CAE methodology.

As depicted in the part D of Fig. 1, a typical roller configuration differs from gerotor only for the presence of roller cylinders that are inserted between the stator and the rotor of the machine and can assure a valuable reduction of friction. For the case here considered, the pinion of the roller motor has 6 teeth, while the annular gear has 7 internal teeth; meaning, that the volume of 42 tooth spaces is delivered per shaft revolution and a large displacement together with reduced volume can be achieved at the same time. In particular, the manifold, C, represents the connecting part between vanes and the valve plate, B. The axial balance of the system is obtained through the common presence of a sealing ring, A, and two springs positioned between the ring and the machine case, where internal leakage flows determine a damping action on the moving parts. As a consequence of this, in the following, a mass-spring-damper model has been introduced in order to account for this phenomenon.

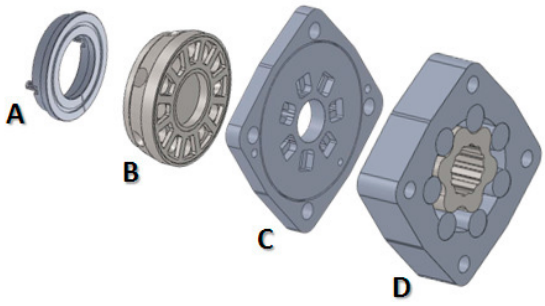

Fig. 1. Main parts of the roller motor.

3. LUMPED AND DISTRIBUTED PERAMETERS MODEL

As already presented in Babbone et al. (2011), the LMS Imagine.Lab AMESim simulation environment has been used for developing a detailed lumped and distributed parameters model of an orbit annular gear machine (Fig. 2). In this case, a simplified approach has been adopted for modelling the internal sealing gaps of the hydraulic motor. More in details, a constant height gap has been considered for the leakage paths between the lateral surfaces of the stator ring, rotor and rollers and the internal surface of the manifold and the height values have been evaluated on the basis of the geometrical tolerances. On the other hand, a non-ideal contact points hypothesis has been introduced for the evaluation of the meshing process between rotor teeth and rollers, and thus the hydraulic resistance of these clearances have been set by considering the relative roughness of the neighbouring surfaces. Moreover, a particular feature of the model is represented by the approach followed for estimating the leakage flow rate between the valve plate and the sealing ring that has been computed considering a variable height clearance, depending on the axial balance between four different contributions: the forces exerted by the springs, the axial thrusts resulting from the pressure distributions acting inside the clearances neighboured by the sealing ring and, respectively, the motor case and the valve plate and the viscous frictions exerted on the valve plate itself.

The results calculated applying this numerical model for a wide range of the main performing parameters, spanning inside the whole operating field of the motor, are summarized in non-dimensional form in Fig. 3. The numerical simulations have been performed feeding the hydraulic motor with a fixed volumetric flow rate and imposing a constant external load, while the rotational speed and the pressure drop

between the inlet and the outlet ports are calculated. In particular, in Fig. 3 the computational results (plotted with continuous and dashed red curves) have been compared with the corresponding experimental measurements (represented by black points) and also the rotational speed and pressure drop percentage errors are shown.

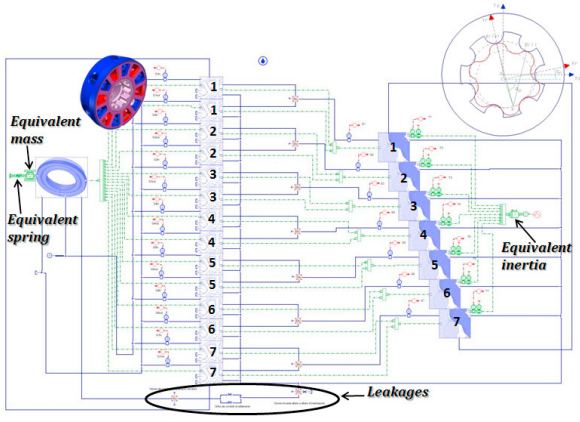

Fig. 2. Sketch picture of the lumped and distributed parameters model.

As far as the numerical vs. experimental comparison proposed in Fig. 3 is concerned, a good reliability of the simplified numerical model can be obtained only for an extremely reduced area of the hydraulic motor operating field, centred around about 40% of maximum motor revving and 50% of maximum exerted torque. On the other hand, the percentage errors become unacceptable outside this operating region, and particularly for higher external loads applied at lowest rotational speeds and when the motor reaches its maximum rotational speed with no exerted torque.

The analysis of this comparison has highlighted a clear negative attitude of the simplified numerical model, mainly due to the constant height approach involved for modelling the motor lateral clearances, that isn't capable to estimate with a sufficient precision the internal leakage flows. A possible way to overcome this problem has been identified in a further enhancement of the computational procedure, based on 2D CFD analysis of the motor internal leakage paths, that will be described in the following.

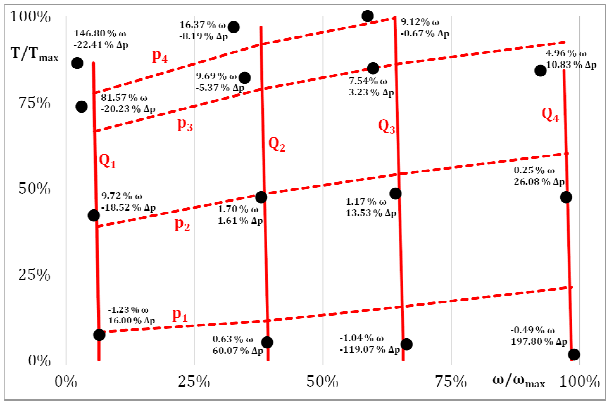

Fig. 3. Numerical vs. experimental comparison for the hydraulic motor simplified numerical model.

4. 2D CFD NUMERICAL APPROACH

In order to increase the effectiveness of the lumped and distributed numerical model for the prediction of the hydraulic motor performance, a 2D CFD numerical procedure, based on the integration of the Reynolds equation, has been developed and applied to the study of the flow field inside the machine lateral clearances. As clearly described by many authors in literature, the pressure distribution and the flow field inside the sealing gaps of hydraulic machines can be determined integrating the Reynolds equation inside clearances bounded by fixed or moving internal components, once boundary conditions are properly imposed to the geometric domain. In particular, for this application, great attention has to be devoted to the determination of the pressure distribution acting inside the volumes sealed between rotor and stator teeth and rollers (the coloured regions in Fig. 4).

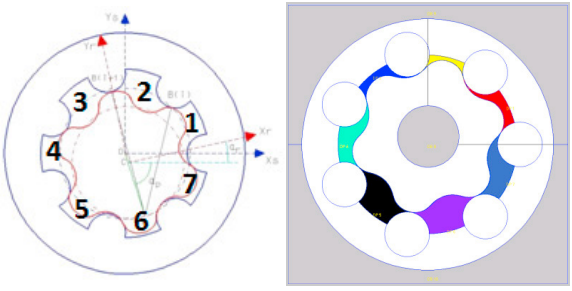

Fig. 4. Reference frame adopted for the volumes sealed between rotor and stator teeth and rollers.

In this case, pressure results computed by the lumped and distributed parameters model have been imposed as boundary conditions for 2D CFD simulations. In Fig. 5, 6 and 7, for example, the non-dimensioned pressure curves calculated for three different operating points of the motor map shown in Fig. 3, and respectively identified with volumetric flow rate and pressure couples (Q_1,p_1), (Q_2,p_2) and (Q_4,p_3), are shown as a function of rotor angular position.

As well shown in Koç et al. (1997a), Koç et al. (1997c), Lasaar (2000), Olems (2000), Huang (2002) and Bassani et al. (1992), under the hypotheses of laminar and isothermal flow of a Newtonian and incompressible fluid, and neglecting the effect of inertial and buoyancy forces, the pressure distribution in the clearances bounded by the lateral surfaces of the stator ring, rotor and rollers and the internal surface of the manifold must satisfy the equation:

$$\vec{\nabla}\cdot\left(h^3\cdot\vec{\nabla}p\right)=6\cdot\mu\cdot\left(\vec{v}\cdot\vec{\nabla}h\right)+12\cdot\mu\cdot\dot{h} \qquad (1)$$

where h is the clearance height, and p, v and μ are, respectively, the fluid pressure, velocity and dynamic viscosity. As shown, (1) details the Reynolds equation once written assuming a negligible contribution of the pressure gradient along the clearance height. With reference to the bi-dimensional, Cartesian, orthogonal coordinate system sketched in Fig. 8, the Reynolds equation becomes:

$$\frac{\partial}{\partial x}\left(\frac{1}{12\mu}\frac{\partial p}{\partial x}h^3\right)+\frac{\partial}{\partial y}\left(\frac{1}{12\mu}\frac{\partial p}{\partial y}h^3\right)=\frac{u}{2}\frac{\partial h}{\partial x}+\frac{v}{2}\frac{\partial h}{\partial y}+\frac{dh}{dt} \qquad (2)$$

being u and v the velocity components along, respectively, x and y directions. Furthermore, once a constant value for the clearance height is assumed, (2), turns into the well-known Laplace form:

$$\nabla^2 p = 0 \tag{3}$$

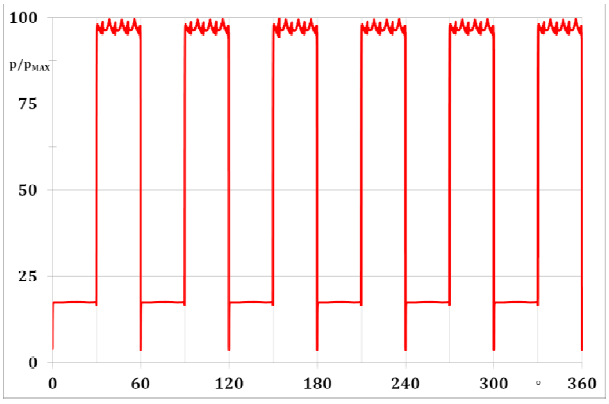

Fig. 5. Non-dimensioned pressure curve for operating point (Q_1, p_1).

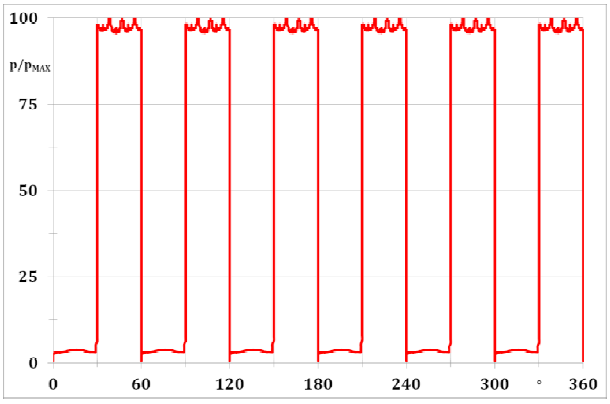

Fig. 6. Non-dimensioned pressure curve for operating point (Q_2, p_2).

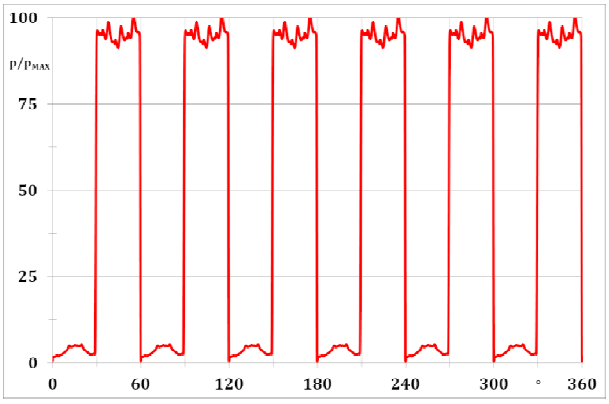

Fig. 7. Non-dimensioned pressure curve for operating point (Q_4, p_3).

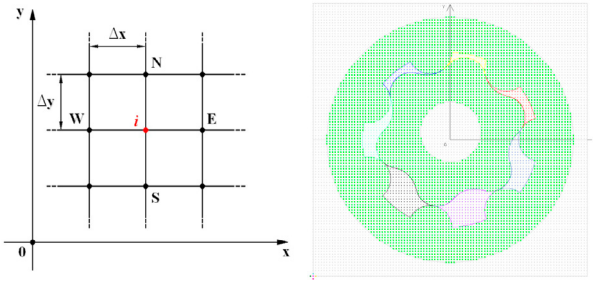

Fig. 8. Reference grid used for calculation and mesh grid of the rotor-stator coupling.

As well known, (2) and (3) can be solved, and they present a unique solution, once proper boundary conditions for pressure are set on the clearance boundaries. In this paper the Reynolds equation has been solved using a finite difference method by replacing, as described in Kreysig (1993), the partial derivatives by second order algebraic approximations.

The discrete schema of solution has been referred to the rectangular grid depicted in Fig. 8, and having nodes uniformly spaced along x and y directions. According to the elementary grid shown in Fig. 8, the pressure first and second order spatial derivatives can be expressed, for the generic node i, as:

$$\left(\frac{\partial p}{\partial x}\right)_i = \frac{p_E - p_W}{2\Delta x} \tag{4}$$

$$\left(\frac{\partial p}{\partial y}\right)_i = \frac{p_N - p_S}{2\Delta y} \tag{5}$$

$$\left(\frac{\partial^2 p}{\partial x^2}\right)_i = \frac{p_E + p_W - 2p_i}{\Delta x^2} \tag{6}$$

$$\left(\frac{\partial^2 p}{\partial y^2}\right)_i = \frac{p_N + p_S - 2p_i}{\Delta y^2} \tag{7}$$

where Δx and Δy are the constant discretization steps, while p_N, p_S, p_W and p_E are the generic grid nodes pressure values (Fig. 8).

Moreover, assuming the clearance boundaries as completely rigid and neglecting the elasto-hydrodynamic effects, according to the experimental measurements detailed in Koç et al. (1997a) and Koç et al. (1997b), a steady-state working condition has been considered, and the second term on the right hand of (1) has been neglected. In this way, the lateral clearance height has been imposed as a geometry dependent parameter and, in order to describe both the variable and the constant clearance configurations, it has been characterized adopting a linear variation along grid directions:

$$h(x, y) = h_0 + m \cdot x + n \cdot y \tag{8}$$

being h_0 the clearance height at the coordinate system origin, O, and m and n the coefficients needed to introduce a relative tilt along, respectively, x and y directions.

This choice allows evaluating the clearance heights spatial derivatives as:

$$\frac{\partial h}{\partial x} = m \tag{9}$$

$$\frac{\partial h}{\partial y} = n \tag{10}$$

The system of algebraic equations thus obtained has been reduced to a non-dimensional form, and it has been solved adopting the stabilized bi-conjugate gradient iterative method (Saad (1996)), specific for large order sparse linear systems.

Moreover, an iterative procedure has been implemented in order to reach the convergence between the results calculated with the lumped and distributed parameters and the multidimensional CFD approach. In particular, the pressure distribution and the flow field computed inside the machine lateral clearance have been used in order to correct the hydraulic resistance of the main leakage paths and these new values permit to progressively increase the reliability of the lumped and distributed parameters model.

5. COMBINED APPROACH NUMERICAL RESULTS

In this paragraph the computational results, obtained when the convergence of the previously introduced iterative procedure has been reached, are presented in terms of hydraulic motor performance map.

In Fig. 9, the numerical vs. experimental comparison, previously shown in Fig. 3, has been updated with the numerical results coming from the iterative combined methodology.

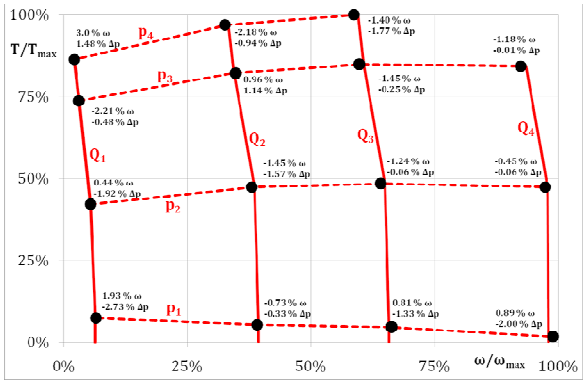

Fig. 9. Numerical vs. experimental comparison updated with the results coming from the iterative combined methodology.

In this case, a significant increase of the model reliability can be appreciated for the machine overall operating range. In fact, a considerable percentage errors reduction, in terms of both predicted rotational speed and pressure drop, is clearly evident and, particularly, for higher external loads applied at lowest rotational speeds and when the motor reaches its maximum rotational speed with no exerted torque, being the maximum absolute values always lower than 3%.

Another important feature of this combined approach is the estimation of the clearance heights mean values per round, illustrated in Fig. 10 for a wide range of the hydraulic motor operating field, as computed for a convergent solution of the iterative procedure.

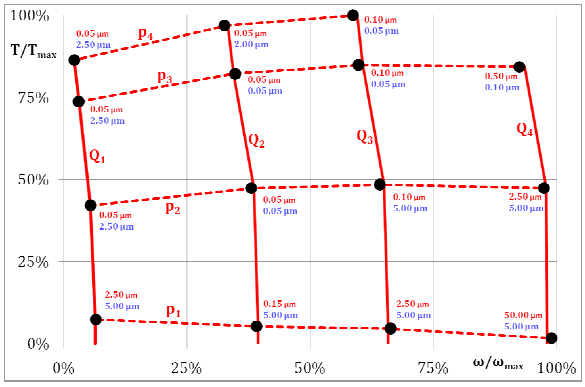

Fig. 10. Clearance heights mean values per round computed for a convergent solution of the iterative procedure.

For this important operating parameter no experimental data were available but the numerical results seem qualitatively consistent and can be very useful in order to understand the main features of the leakage paths hydrodynamic lubricating mechanism.

6. CONCLUSIONS

In this paper an innovative computational approach, useful for predicting the performance of orbit annular machines, has been proposed and validated through a detailed numerical versus experimental comparison. More in details, an iterative procedure, based on both lumped and distributed numerical modelling and 2D CFD simulations, has been built up and applied to the study of a typical hydraulic roller motor for a wide range of operating conditions, in terms of both rotational speed and exerted torque.

The numerical results obtained for convergent solutions have been found in very good agreement with the experimental measurements and percentage errors always lower than 3% clearly demonstrate the consistency of this novel approach. Moreover, the analysis of the 2D CFD pressure distributions acting on the stator, rotor and rollers lateral surfaces have been very useful in order to estimate the motor internal leakages and to understand its axial balancing mechanism. In this way, the predictive capability of the lumped and distributive numerical model have been increased and optimized geometrical solutions for the main machine inner components can be designed and verified.

REFERENCES

Babbone, R., Bottazzi, D., Cagni, G., Grasselli, F., and Milani, M. (2011). CAE design of orbit annular machines. *12th Scandinavian International Conference on Fluid Power,* Tampere (Finland), May 18-20, 2011.

Bassani, R. and Piccigallo, B. (1992). *Hydrostatic lubrification*. Elsevier.

Bonacini, C. and Carra, R. (1987). A numerical method to evaluate axial force in pressure compensated gears pumps and motors. *Proceedings of the 43rd Annual Meeting, National Conference on Fluid Power, NFPA,* Chicago (USA), October 11-13, pp. 403-408.

Edge, K., Keogh, P., and Eaton, M. (2001). Modelling and simulation of pressures within the meshing teeth of gear pumps. *International Conference on Recent Advances in Aerospace Actuation Systems and Components,* Toulouse (France), June 13-15, 2001.

Gutés, M., Gámez Montero, P.J., Castilla, R., and Codina Macià, E. (2000). Journal bearing performance in gear pumps. *Proceedings of the 1st International FPNI Ph.D. Symposium on Fluid Power,* Hamburg (Germany), September 20-22, 2000, pp. 259-269.

Huang, C. (2002). Gap flow investigation of the piston cylinder assembly in axial piston pumps considering EHD effects. *Proceedings of the 2nd International FPNI Ph.D. Symposium on Fluid Power,* Modena (Italy), July 3-6, 2002.

Ivantysyn, J. and Ivantysynova, M. (2003). *Hydrostatic pumps and motors*. TBI Edition.

Koç, E., Kurbant, A.O., and Hooke, C.J. (1997). An analysis of the lubrication mechanisms of the bush-type bearings in high pressure pumps. *Tribology International,* Vol. 30 (Num. 8), pp. 553-560.

Koç, E. and Hooke, C.J. (1997). An experimental investigation into the design and performance of hydrostatically loaded floating wear plates in gear pumps. *Wear,* Num. 209, pp. 184-192.

Koç, E. and Hooke, C.J. (1997). Considerations in the design of partially hydrostatic slipper bearings. *Tribology International,* Vol. 30 (Num. 11), pp. 815-823.

Kreysig, E. (1993). *Advanced engineering mathematics.* John Wiley & Sons.

Lasaar, R. (2000). The influence of the microscopic and macroscopic gap geometry on the energy dissipation in the lubricating gaps of displacement machines. *Proceedings of the 1st International FPNI Ph.D. Symposium on Fluid Power,* Hamburg (Germany), September 20-22, 2000, pp. 101-116.

Mancò, S. and Nervegna, N. (1989). Simulation of an external gear pump and experimental verification. *JHPS International Symposium on Fluid Power,* Tokio (Japan), March 1989, pp. 139-152.

Mancò, S. and Nervegna, N. (1993). Pressure transients in an external gear hydraulic pump. *JHPS International Symposium on Fluid Power,* Tokio (Japan), March 1993, pp. 221-227.

Merrit, H.E. (1966). *Hydraulic control system.* John Wiley & Sons.

Olems, L. (2000). Investigations of the temperature behaviour of the piston cylinder assembly in axial piston pumps. *International Journal of Fluid Power,* Num. 1, pp. 27-38.

Poy Ferrer, M. and Codina Macià, E. (2002). Suction capability of gear pumps. *Proceedings of the 2nd International FPNI Ph.D. Symposium on Fluid Power,* Modena (Italy), July 3-6, 2002.

Saad, Y. (1996). *Iterative methods for sparse linear equations.* PWS Publishing Company.

Wieczorek, U. (2000). Simulation of the gap flow in the sealing and bearing gaps of axial piston machines. *Proceedings of the 1st International FPNI Ph.D. Symposium on Fluid Power,* Hamburg (Germany), September 20-22, 2000, pp. 493-507.